

Chapter 5:

*Selective oxidation of ethane to acetic
acid over MoVAlO_x based catalytic system
with molecular oxygen*

5.1 Introduction

Research activity on the selective oxidation of lower alkanes, especially C₂-C₄ alkanes, to the corresponding alkenes or oxygenates (acetic acid, acrylic acid, etc) has gained a high momentum in recent years [1, 2]. Selective oxidation of lower alkanes is an attractive path towards the chemical utilization of cheap natural gas resources. For instance, one-step direct oxidation of ethane and propane to acetic acid and acrylic acid, respectively, is an alternative method to the currently employed alkene based routes [2-5]. Generally, lower alkanes are less reactive due to the non-availability of a lone pair electrons and little polarity of the C-H bonds, and hence, their oxidation is usually encountered with difficulties. Furthermore, a high selectivity to the required products is obtained generally at low conversion. Higher conversion invariably leads to less selective to the required products, due to the formation of thermodynamically stable, undesirable combustion products. In spite of the above limitation, a great deal of efforts have been attempted to achieve selective functionalization of lower alkanes. However, in the case of selective oxidation of ethane only a few catalysts are known that are efficient in terms of acetic acid and ethylene yield at a relatively mild experimental condition [1, 2, 6].

Oxidation of ethane involves several micro intermediate steps that demand a multifunctional catalyst. Thus, the selection of a suitable catalyst containing many active phases (multifunctionality) for the ethane oxidation and maximizing the selectivity to ethylene and/or acetic acid under appropriate operating condition is a complex and challenging task. Several research groups have studied a broad spectrum of catalysts using various techniques to understand the active sites responsible for the selective oxidation of ethane. However, the knowledge available on the reaction mechanism is still rather limited and hence there is a need for systematic studies on the wide range of catalyst systems in order to understand the structure-activity correlations [2, 7, 8].

There have been many reports emphasizing the importance of elements like Te and Nb ions along with Mo-V containing basic composition for the formation/stabilization of the active phases responsible for the selective oxidation of ethane [1, 5, 10, 11]. Reports are also available indicating the importance of the initial elemental composition, the pH, the preparation methodologies and the treatment temperatures for a better yield of the required alkenes and oxygenates, however, these dependencies vary with catalyst to catalyst [4, 6].

The initial report on MoVAIO_x by Ueda *et al* at an atmospheric pressure and at 340 °C showed less than 4 mol % ethane conversion with a low selectivity to acetic acid [12]. In the present paper, we report on the catalytic activity of MoVAIO_x type catalysts for the selective oxidation of ethane to produce ethylene and acetic acid at moderate ethane conversion, as a function of the pH of the preparative gel of the catalysts synthesized. MoVAIO_x type catalysts prepared at different pH conditions were also tested at different experimental conditions *viz.* pressure, temperature and ethane/O₂/H₂O feed ratios in order to obtain acetic acid and ethylene in high yield. Interestingly, the catalyst prepared from a gel at pH 2 was found to have superior activity than other catalysts. We have also identified different phases present in the catalysts prepared at different pH conditions. Structure-activity correlations were made based on the detailed characterization of the catalysts by powder XRD, Raman, UV-visible, and EPR spectral techniques.

5.2 Experimental

5.2.1 Catalyst preparation and Characterization

Catalyst composition of general formula MoVAIO_x with a preparative composition of the elements Mo, V and Al in the atomic ratio 1.0:0.333:0.167 respectively was synthesized using a hydrothermal method [12]. Anderson type heteropoly molybdate, (NH₄)₃AlMo₆H₆O₂₄.7H₂O, prepared from the mixed aqueous solution of ammonium heptamolybdate and aluminum sulfate [12, 13] and was used as a source for Mo and Al. Typically, the catalyst compositions of MoVAIO_x were prepared as follows: aqueous solutions of (NH₄)₃AlMo₆H₆O₂₄.7H₂O and VOSO₄ were mixed at room temperature, the slurry was adjusted to the required pH value (1, 2, 3 or 4) using NH₄OH or HNO₃ and the final mixture was transferred to a PTFE lined autoclave (200 ml capacity). The autoclave was heated to 175 °C for 48 h under constant rotation (40 rpm). After 48 h, the autoclave was cooled and the dark solid mass obtained at the bottom of the autoclave was separated from the solution, washed with water several times and dried at 100 °C overnight in an oven. The final catalyst compositions were named as MoVAIO_x-1, MoVAIO_x-2, MoVAIO_x-3 and MoVAIO_x-4, where the numerical values indicate the pH at which the catalysts were prepared.

The bulk compositions of Mo, V and Al were analyzed by ICP using a Plasma 400 Perkin Elmer spectrometer and their surface composition was done using EDX method. The surface area of the catalysts was determined by N₂ adsorption at 77 K,

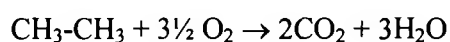
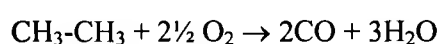
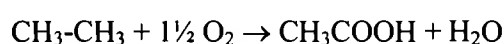
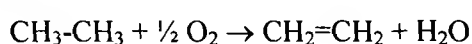
using the multipoint BET analysis method with an Autosorb-1 Quantachrome flow apparatus. The catalysts were dehydrated in vacuum at 250 °C for 10 h prior to the measurements. The room temperature powder X-ray diffraction (XRD) patterns of calcined catalysts were collected on a Philips X'Pert Pro 3040/60 diffractometer using Cu K α radiation ($\lambda = 1.5418\text{\AA}$), nickel filter and X'celerator as detector which employs the real time multiple strip (RTMS) detection technique. XRD patterns were collected in the 2θ range 5 -75° steps of 0.017°. Scan type was the continuous scanning mode and the scan time per step was 50 s. Scanning electron microscopy (SEM) and EDX microanalyses were performed on a JEOL JSM 6300 LINK ISIS instrument.

The FT-IR and Raman spectra of the catalysts were recorded on a Shimadzu FTIR 8201 PC instrument and Ranishaw 2000 Raman Microscope excited with 633 nm Laser respectively. Diffuse reflectance UV-visible spectra were collected on a Perkin Elmer Lambda 900 series, equipped with a 'Praying Mantis' attachment from Harrick. The spectra were recorded for VOSO₄, MoO₃, V₂O₅ and the as-synthesized and calcined (NH₄)₃AlMo₆H₆O₂₄·7H₂O (hereafter referred as Mo₆Al-AS and Mo₆Al-Cal respectively) as references for the analysis. The electron paramagnetic resonance (EPR) spectra were recorded at room temperature on a Bruker EMX X-band spectrometer operating at 100 kHz field modulation. The microwave frequency was calibrated using a frequency counter of the microwave bridge ER 041 XG-D. Bruker Simfonia and WINEPR software packages were used in the spectral simulations and to calculate hyperfine coupling constant.

5.2.2 Catalytic activity testing

The ethane oxidation experiments were performed in a typical laboratory fixed bed reactor using a corrosion resistant stainless steel tubular reactor of internal diameter of 9 mm and 450 mm height which was kept in a tubular furnace. The catalyst (0.3-0.5 mm particle size) was introduced in the reactor and diluted with 2-4 g of silicon carbide with similar in size in order to keep a constant volume in the catalyst bed. A thermocouple was installed in the center of the catalyst bed in contact with the catalyst particles to measure the reaction temperature. The heating zones at the inlet and the outlet of the reactor were filled with inert porcelain particles. The catalyst was activated by heating the reactor to 350 °C at a heating rate of 2 °C/min

under air flow for 4 h and then to 400 °C under He flow for 4 h. The reactor was then brought to the required temperature, and pressurized to the required level with a feed using a back pressure controller placed on the reactor outlet stream. A typical composition of the feed was ethane/air/steam: 27.6/47.6/24.8 mol %. The water (steam) feed was preheated at 250 °C and then thoroughly mixed with the other gas feed prior to their contact with the catalyst. The flow rate was varied (from 40 to 100 ml/min) in order to achieve different ethane conversion levels. Experiments were carried out at temperatures in the range 250-350 °C to achieve the highest combined selectivity for ethylene and acetic acid at a moderate ethane conversion. The liquid products (mainly acetic acid and water) were separated from the gas products by an ice cold condenser, collected in high pressure liquid-gas separator and analyzed using offline gas liquid chromatography (GC: HP 5890 series 11 using a 1.5 m by 3 mm column packed with material sold under the trademark PORAPAQTM-QS). Acetic acid was also estimated by standard volumetric titration method. The gas products were analyzed online by gas chromatography (GC: Chemito 1000) operating with three columns. Oxygen, nitrogen and carbon monoxide were analyzed using a 2.5 m by 3 mm column of 13X molecular sieve. Carbon dioxide, ethane and ethylene were analyzed using a 0.5 m x 3 mm column packed with material sold under the trade name PORAPAQTM-N. The carbon balance was in the range 93-97 %. In all cases, the conversion and selectivity calculations were based on the following stoichiometries:



The selectivity data were calculated on the basis of product sum. Details of the reaction conditions are described in the footnotes of the Tables and Figures. The conversion of ethane in an experiment using an empty volume reactor (blank run) was lower than 1 %, confirming that the homogeneous reaction is negligible at the experimental conditions employed for the present catalytic activities.

5.3 Results

5.3.1 Synthesis and Characterization

5.3.1.1 Synthesis, elemental composition and surface properties

The elemental composition of catalysts of general formula MoVAIO_x prepared hydrothermally at four different pH values and the yield of the final catalysts (calcined catalysts) are given in Table 1. The catalyst yield was found to decrease at higher pH condition as seen in the Table 1. The bulk elemental composition of the catalysts was obtained from ICP analysis. The data clearly indicate that the final composition of the catalyst is different from the initial preparative composition depending on the pH values. Also, Mo/V and Mo/Al molar ratios decrease with increase in pH indicating that the Mo content is lower at the higher pH value.

The surface elemental composition for all the catalysts was determined by EDX method (Table 1) and it was found that these elemental compositions are different from the bulk composition. The amount of vanadium at the surface of the catalysts was higher as compared to that of the bulk except with the MoVAIO_x-4 catalyst, indicating its mobility to the surface of the catalysts. BET surface area measurements have also been carried out for these catalysts and the data are presented in Table 1. The surface area of the catalyst MoVAIO_x-1 was 7 m²/g, while for the other catalysts it was in the range 16- 17 m²/g.

Table 1: Elemental compositions and surface properties of hydrothermally synthesized MoVAIO_x catalysts prepared at different pH values.

Catalyst	^a Yield, %	Elemental Composition		
		ICP Analysis	EDX Analysis	Surface area, m ² /g
MoVAIO _x -1	99	Mo ₁ V _{0.15} Al _{0.20} O _x	Mo ₁ V _{0.26} Al _{0.11} O _x	6
MoVAIO _x -2	96	Mo ₁ V _{0.34} Al _{0.09} O _x	Mo ₁ V _{0.36} Al _{0.30} O _x	16
MoVAIO _x -3	33	Mo ₁ V _{0.7} Al _{0.28} O _x	Mo ₁ V _{0.78} Al _{0.69} O _x	17
MoVAIO _x -4	13	Mo ₁ V _{1.75} Al _{0.49} O _x	Mo ₁ V _{1.27} Al _{1.05} O _x	17

^a Yield of calcined catalysts, calculated on the basis of concentration of Mo with respect to initial elemental composition taken for the synthesis

5.3.1.2 Powder X-Ray diffraction

The powder XRD patterns of the four calcined catalysts prepared at different pH values can be seen in Figure 1. The calcination was carried out at 400 °C under N₂ after treating the catalysts in air up to 350 °C for 2 h. The catalysts MoVAIO_x-1 and MoVAIO_x-2 showed a similar XRD patterns exhibiting predominantly MoO₃ [JCPDS, 76-1003] and MoV₂O₈ [JCPDS, 74-1510] phases. Although, the quantification of different phases was not carried out, the relative intensity of MoO₃ is much higher in MoVAIO_x-1. Relative amount of MoV₂O₈ phase was higher in MoVAIO_x-2 compared to MoVAIO_x-1. In other words, the relative intensity ratio of [MoV₂O₈]/ [MoO₃] is higher in MoVAIO_x-2 than in MoVAIO_x-1. In addition, traces of Mo₄O₁₁ [JCPDS, 13-0142], a reduced phase, is also seen in both catalysts (which is more prominent in MoVAIO_x-2). The XRD pattern of MoVAIO_x-3 exhibits MoV₂O₈ as a major phase along with a minor phase of Mo₄V₆O₂₅ [JCPDS, 34-0530]. Interestingly, MoO₃ phase is totally absent in MoVAIO_x-3. In addition, low intensity peaks were seen at 2θ values 17.63(23)°, 29.51(15)°, 38.12(3) and 46.19(12)° could not be fitted with any of the known single phases. For MoVAIO_x-4, the pattern was dominated by V₂O₅ [JSPDS, 85-0604] phase as a major phase along with a medium intensity Mo₄O₁₁ and MoVAIO₄ [JSPDS, 89-0871] phases. A trace amount of Mo₄V₆O₂₅ phase was also seen in MoVAIO_x-4.

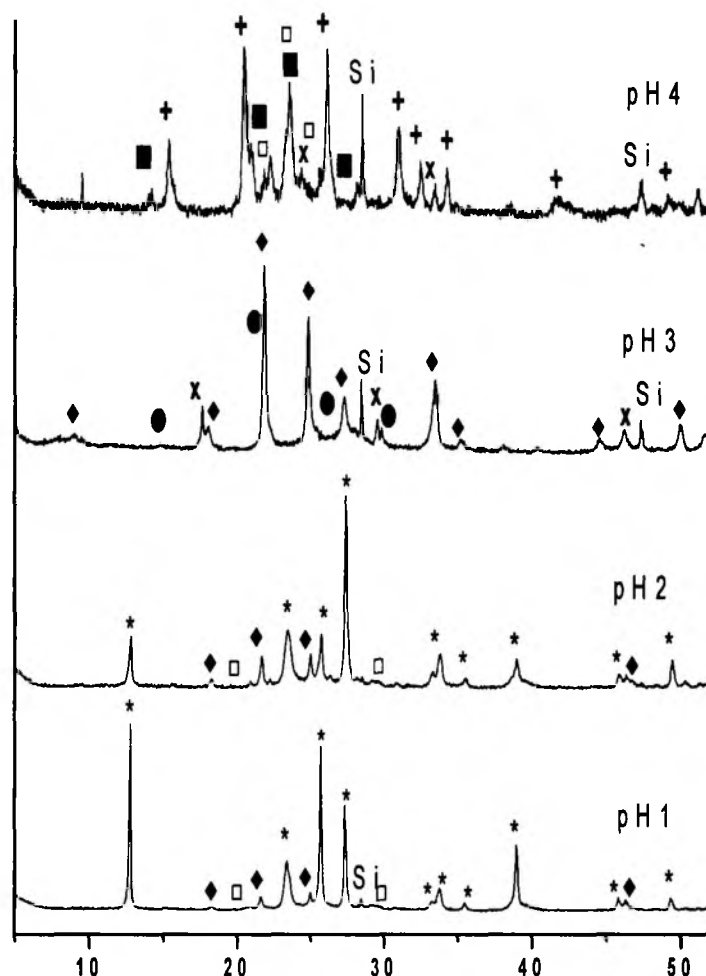


Figure 1: Powder XRD pattern of the catalyst. *: MoO₃, ◆: MoV₂O₈, □: Mo₄O₁₁, +: V₂O₅, ●: Mo₄V₆O₂₅, ■: MoVAIO₇, x: unidentified phase, Si: silicon standard.

5.3.1.3 Morphology of MoAlVO_x catalysts

The morphology of calcined catalysts was investigated by SEM analysis. All the four catalysts were found to have completely different morphologies and the images are given in Figure 2. Long rod or needle shaped crystals with a length about 4-40 μm were observed in the case of MoVAIO_x-1. These needle or rod shaped crystals have collapsed into smaller sizes in MoVAIO_x-2 catalyst as shown in the Figure 2. For the catalysts prepared at higher pH values viz., MoVAIO_x-3 and MoVAIO_x-4, the images are more of microcrystalline and spongy in nature respectively.

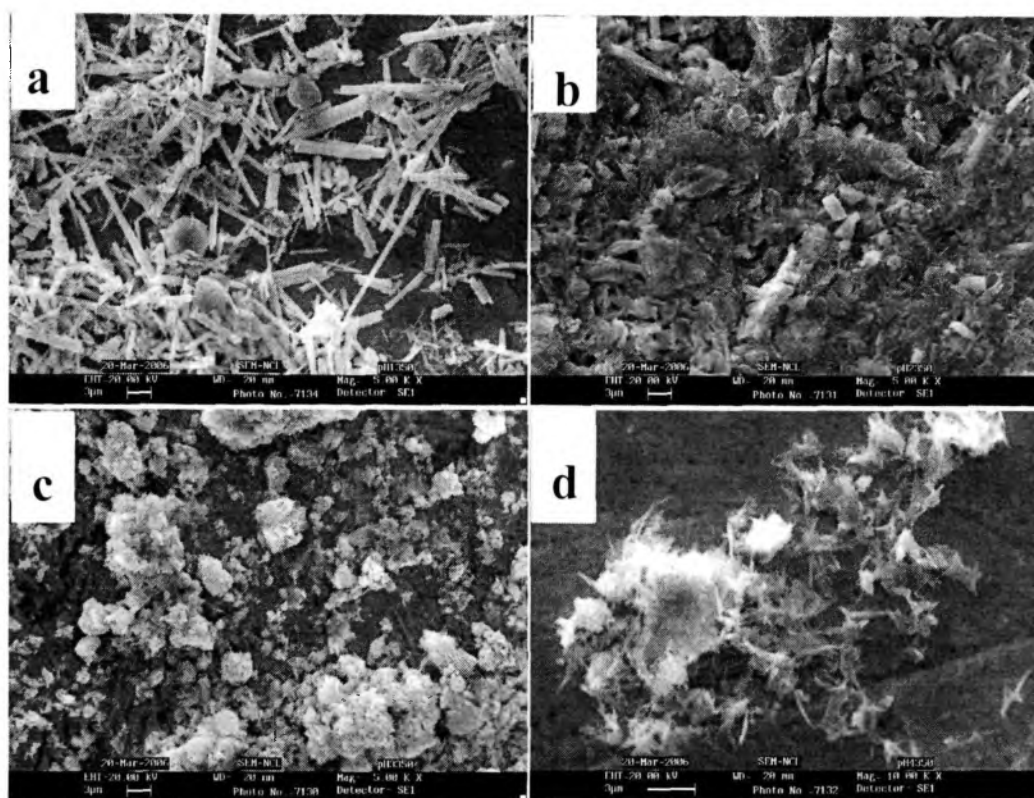


Figure 2: SEM images of (a) MoVAIO_x-1, (b) MoVAIO_x-2, (c) MoVAIO_x-3 and (d) MoVAIO_x-4

5.3.1.4 Raman Spectroscopy

Raman spectroscopy was used to identify different moieties/phases having different coordination symmetry present in the catalytic catalysts. The Raman spectra of all the calcined catalysts recorded at room temperature are shown in Figure 3. The spectra of MoVAIO_x-1 and MoVAIO_x-2 catalysts showed bands at 992, 820, 664 cm⁻¹ which are characteristic of α -MoO₃ species and its presence was also supported by the XRD data.

A broad shoulder band around 700 cm⁻¹ and a peak at 992 cm⁻¹ (the latter band might be overlapped with that of α -MoO₃) indicate the presence of phases containing V₂O₅ unit *viz.* MoV₂O₈ phase [14]. Interestingly, for MoVAIO_x-3 and MoVAIO_x-4 catalysts, the intensity of 820 cm⁻¹ band diminished to a broad shoulder. However, the band centered around 700 cm⁻¹ increased many fold and became a broader band for MoVAIO_x-4 catalyst. The above features indicate the absence or negligible amount of α -MoO₃ species and increased amount of pure V₂O₅/ (V₂O₅- containing phases e.g.

MoV₂O₈) in these catalysts. This is quite understandable as the relative amount of vanadium content was higher in this catalyst compared to the catalysts prepared at a low pH. In the case of MoVAIO_x-4, the V content was more than that of Mo as seen in Table 1. The bands at 900 and 850 cm⁻¹ are generally attributed to the stretching mode of Mo-O-Mo bonds of polymerized surface molybdenum oxide containing species in different configurations (dimers, oligomers) [15, 16]. The broad bands centered around 920, 900 and 850 cm⁻¹ are attributed to crystalline Mo₄O₁₁ and Mo₄V₆O₂₅ species in addition to MoO₃ type compounds. The spectra of all catalysts showed a broad band in the region 700-675 cm⁻¹ (which were stronger in MoVAIO_x-3 and MoVAIO_x-4) and a band around 400 cm⁻¹. These bands are assigned to V-O-V (or V-O-Mo) stretching vibrations of polymeric surface species e.g. MoVAIO₄, Mo₄V₆O₂₅ etc [17]. The bands can also be partly attributed to the presence of a bulk V₂O₅ especially for MoVAIO_x-4 catalyst as characteristic bands of V₂O₅ appear at 282, 405, 695 and 993 cm⁻¹ [14]. The absence of 760 or 937 cm⁻¹ band in all the catalysts indicates that monomeric tetrahedral vanadate species (~760 cm⁻¹) and surface metavanadate species (937 cm⁻¹) are either absent or present in negligible quantities [18]. An isolated monovanadate group having terminal V=O stretching mode which generally exhibits a distinct narrow band at 1030-1020 cm⁻¹, is absent in the catalysts [14, 19]. Also, bands associated with AlVO₄ (characteristic bands are: 1003, 970, 943 cm⁻¹) are absent in the calcined catalysts [20].

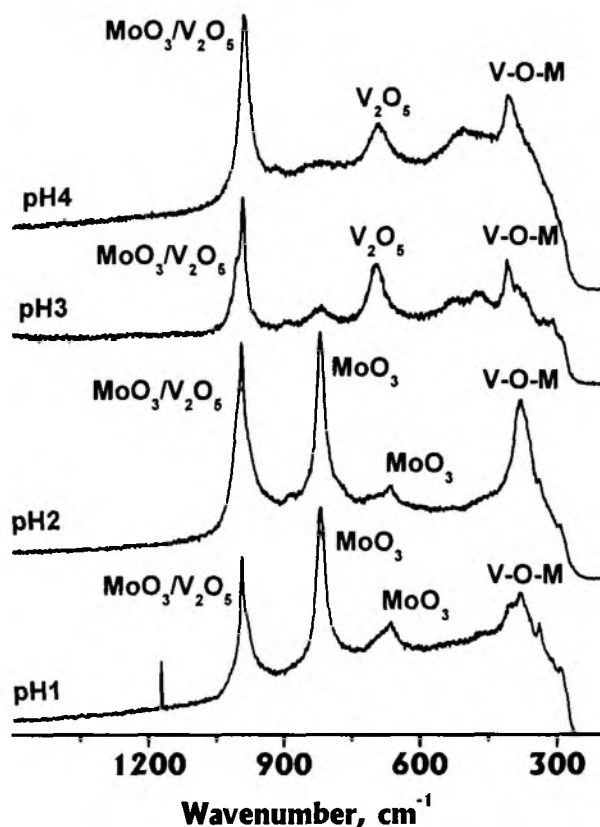


Figure 3: Raman spectra of (a) MoVAIO_x-1, (b) MoVAIO_x-2, (c) MoVAIO_x-3 and (d) MoVAIO_x-4 (calcined samples)

5.3.1.5 UV-visible spectroscopy

The diffuse reflectance UV-visible spectra of the calcined catalysts prepared at different pH values were recorded at room temperature and are shown in Figure 4. The spectra were deconvoluted to identify different bands present especially in the region 200-500 nm. Accordingly, the spectra could be deconvoluted into five major bands centered on 234, 265, 307, 376, 452 nm and however, their intensities vary with catalysts prepared at different pH. The UV-visible spectra of few reference catalysts namely VOSO₄, V₂O₅, MoO₃ as well as, as synthesized and calcined (NH₄)₃AlMo₆H₆O₂₄·7H₂O catalysts; represented by Mo₆Al-AS and Mo₆Al-Cal respectively were also recorded for comparison and the spectra are shown in Figure 5.

The UV-visible spectra of all the calcined catalysts were dominated by five major peaks centered around 234, 265, 307 (br), 376, 452 (vs) nm and also a broad band above 500 nm. The intensity of the bands centered on 234, 265 and 307 nm was

stronger and the peaks at 376 and 452 nm appear as a shoulder for the catalysts. While the relative intensity of 234 and 265 nm bands are more or less same for both MoVAIO_x-2 and MoVAIO_x-1, bands in the region 305-480 nm became stronger for MoVAIO_x-2. The features of MoVAIO_x-3 and MoVAIO_x-4 were almost similar and the bands in the region 305-480 nm became more intense and a broad shoulder at 452 nm became clearly visible.

The bands in the range of 230-310 nm present in all the catalysts were assigned to Mo⁶⁺ in octahedral coordination with different structural arrangement [5, 18, 19, 21]. The above assignment was further substantiated by the UV-visible spectra of the reference catalysts namely MoO₃, Mo₆Al-AS and Mo₆Al-Cal catalysts (Figure 5) and their spectra are dominated by characteristic bands in the region 200-350 nm. The broad bands appeared above 550 nm are assigned to a *d-d* band associated with Mo and V ions with lower oxidation states e.g. Mo⁵⁺/Mo⁴⁺ or V⁴⁺/V³⁺ as they are expected to exhibit bands in the region 400-750 nm [22]. The above assignments were further supported by comparing the spectra of reference samples, Mo₆Al-Cal and VOSO₄, which have a substantial amount of Mo⁵⁺ and V⁴⁺ respectively, showing characteristic of *d-d* band above 500 nm. The dominant band centered on 376 nm in all the calcined catalysts were assigned to penta coordinated V⁵⁺ [5, 18, 19]. The assignment was also confirmed by comparing with the UV-visible spectrum of reference V₂O₅ catalyst where the vanadium is in five coordination state. The intensity of the above band increases at higher pH values due to the increase in V content at higher pH.

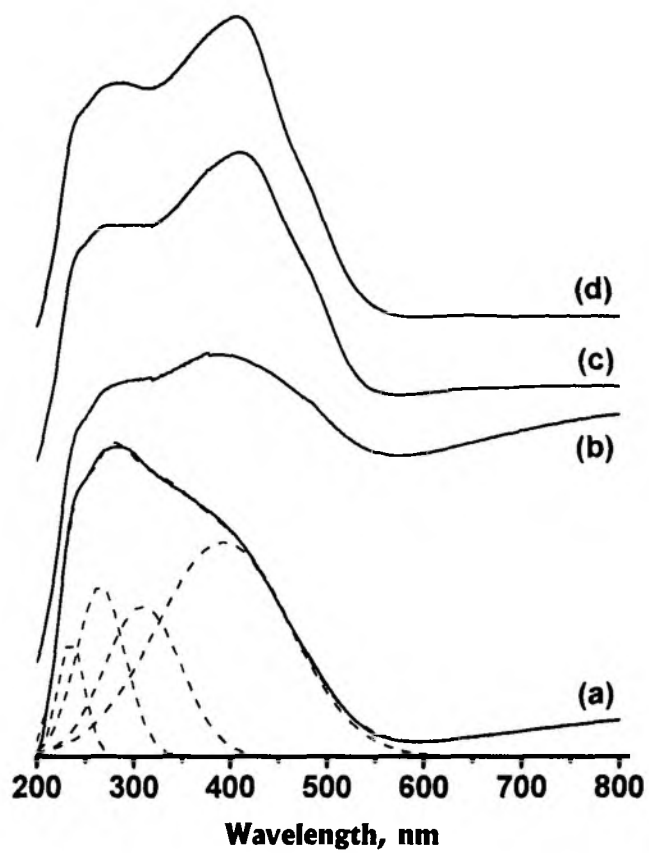


Figure 4: DRS UV-visible spectra of (a) MoVAIO_x-1, (b) MoVAIO_x-2, (c) MoVAIO_x-3 and (d) MoVAIO_x-4 (calcined samples)

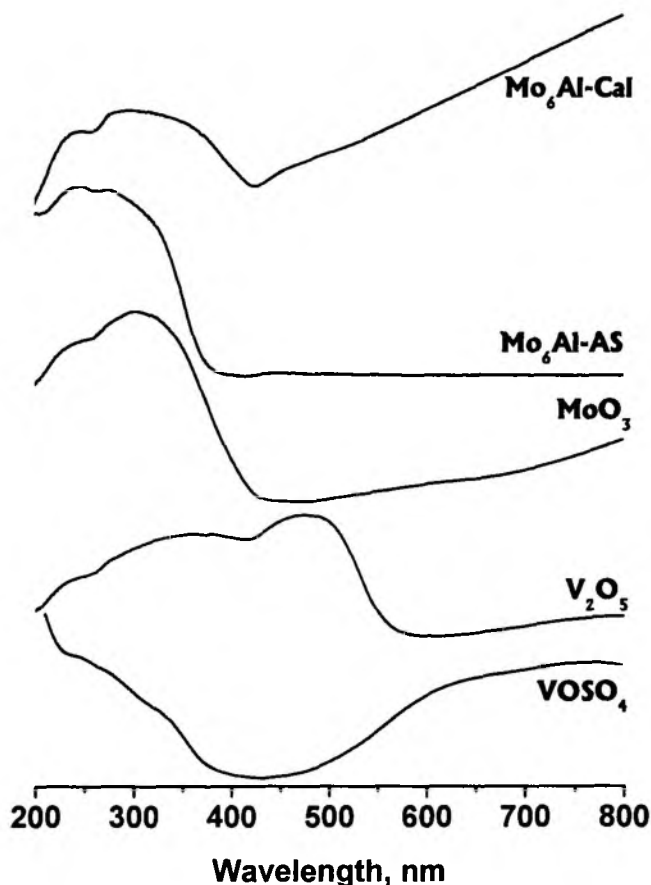


Figure 5: DRS UV-visible spectra of different standard samples

5.3.1.6 EPR Spectroscopy

Figure 6 shows the EPR spectra of all the four calcined catalysts were recorded at room temperature. While the EPR spectra of MoVAIO_x-1 and MoVAIO_x-2 catalysts showed overlapped signals corresponding to Mo⁵⁺ and V⁴⁺, MoVAIO_x-3 and MoVAIO_x-4 catalysts gave signals corresponding to mainly of Mo⁵⁺ with no trace of V⁴⁺ signal. The EPR spectra of V⁴⁺ centers are characteristic of an axial symmetry typical for orthogonal geometry [23]. The EPR spectra of V⁴⁺ of MoVAIO_x-1 and MoVAIO_x-2 were best fitted with Hamiltonian parameters, $g_{\parallel} = 1.926$, $g_{\perp} = 1.985$, $A_{\parallel} = 183$, $A_{\perp} = 53$ at operating microwave frequency, 9.457 GHz.

Normalization of the simulated spectrum with the parallel components of V⁴⁺ EPR signal clearly showed that EPR spectra of MoVAIO_x-1 and MoVAIO_x-2 consist of overlapped signals from V⁴⁺ and Mo⁵⁺ species. EPR spectrum of Mo⁵⁺ showed

unresolved broad isotropic pattern (peak to peak line width of 90 G). The assignment of the EPR signal to Mo⁵⁺ was also substantiated by that of the reference catalyst, Mo₆Al-Cal, which showed a characteristic Mo⁵⁺ signal with 70 G line width (Figure 6). The broad line width may be due to the presence of more than one Mo⁵⁺ sites and/or due to magnetic interactions between the paramagnetic Mo⁵⁺ centers those are in close proximity. In order to quantify the amount of paramagnetic centers viz., V⁴⁺ and Mo⁵⁺, with respect to the total V and Mo contents respectively, the area under the peak of all the EPR spectra (double integration) was calculated using vanadyl sulfate as a standard.

Accordingly, V⁴⁺/V_{total} was estimated to be around 0.8 % in MoVAIO_x-1 as well as MoVAIO_x-2 whereas Mo⁵⁺/Mo_{total} was around 2.5 % for all the catalysts indicating that the majority of Mo and V species are in their higher oxidation states namely Mo⁶⁺ and V⁵⁺ respectively which are diamagnetic. For MoVAIO_x-1 and MoVAIO_x-2 catalysts, the area corresponding to V⁴⁺ was determined separately based on the simulation before estimating the Mo⁵⁺ content.

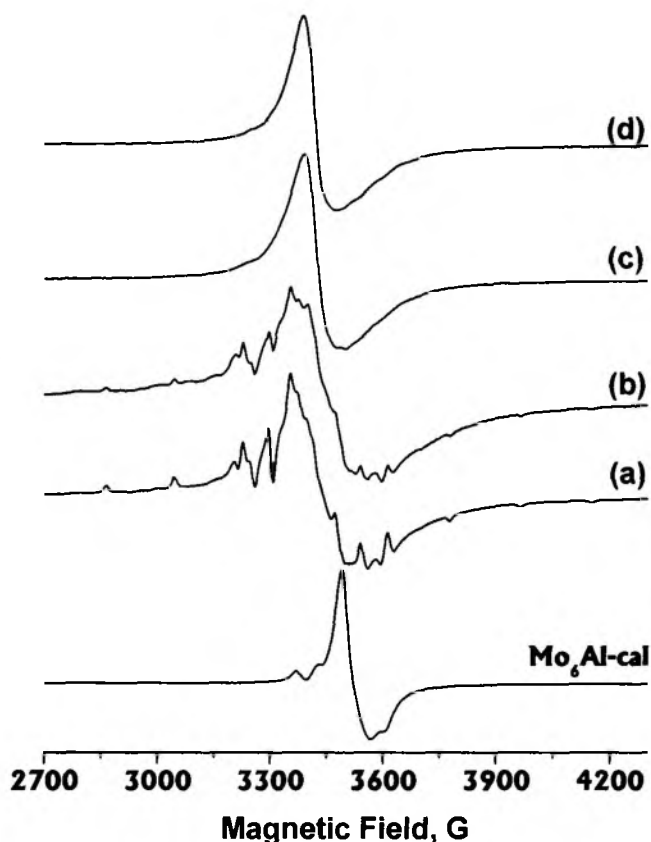


Figure 6: EPR of (a) MoVAIO_x-1, (b) MoVAIO_x-2, (c) MoVAIO_x-3, (d) MoVAIO_x-4 and Mo₆Al-CAL (calcined samples)

5.3.2 Selective Oxidation of ethane

All the four catalysts were tested for selective oxidation of ethane in a fixed bed reactor as described in the experimental section. The reaction was carried out typically at the experimental condition of 300 °C and 15 bar with a flow rate of 48.33 ml/min using ethane/air/steam: 27.6/47.6/24.8 mol % over 2 g of catalyst loading. The reaction was allowed to run for several hours (~ 10 h) to attain saturation and then the products were analyzed for every 3 h and the results are summarized in Table 2. Each data point is an average of three measurements. In all these cases, acetic acid and ethylene were the main products apart from CO and CO₂. Other products like ethanol, methanol and acetaldehyde were also seen but in less than 150 ppm level and are not discussed further. As seen in Table 2, MoVAIO_x-1 gave 30 mol % selectivity to acetic acid and 32 mol % selectivity to ethylene at the ethane conversion of 9.7 mol %.

Interestingly, MoVAIO_x-2 showed an excellent activity with 23 mol % ethane conversion with a combined ethylene and acetic acid selectivity of 80.6 mol % where acetic acid selectivity alone was 40.2 mol %.

MoVAIO_x-3 showed a moderate ethane conversion (10.5 mol %) with a better acetic acid selectivity of 46 mol % where the combined ethylene and acetic acid selectivity of 82 mol %. In both MoVAIO_x-2 and MoVAIO_x-3 catalysts, the selectivity to CO and CO₂ was very low. The catalyst MoVAIO_x-4 showed the least activity of 8.2 mol % ethane conversion with lowest acetic acid selectivity of 3 mol % where selectivity to ethylene was 18 mol % and selectivity to CO_x was 79 mol %. MoVAIO_x-2 gave highest acetic acid yield of 9.25 mol % while MoVAIO_x-4 gave the least yield (0.25 mol %). The other catalysts viz., MoVAIO_x-1 and MoVAIO_x-3 gave an acetic acid yield of 2.91 and 3.78 mol % respectively as shown in Table 2.

Since MoVAIO_x-2 showed a better activity towards ethane oxidation than the other catalysts, MoVAIO_x-2 catalyst was alone tested at different experimental conditions to understand their effects on the ethane conversion and the products selectivity. Experiments were carried out at different reaction pressures in the range 5-20 bar with a feed of ethane/air/steam: 27.6/47.6/24.8 mol % at reaction temperature 300°C and the results are plotted in Figure 7. The reaction pressure has a definite influence on ethylene and acetic acid selectivity. As seen in the Figure, there is a gradual increase in the ethane conversion with increase in the reaction pressure and reached nearly a plateau above 15 bar pressure. The ethane conversion was around 8 % at 5 bar and increased to 23 % at 15 bar. The acetic acid selectivity was around 20 % and the ethylene selectivity was around 73 % at 5 bar and both reached around 40 % at 15 bar pressure and thereafter, the selectivity of ethylene and acetic acid were more or less the same until 20 bar pressure. Thus, the optimum reaction pressure was around 15 bar at 300°C. The variation in the selectivity to CO and CO₂ was small as compared to that of ethylene and acetic acid where the selectivity to CO was slightly higher than that of CO₂. Selectivity to CO was around 5 % at 5 bar which reached around 11 % at 20 bar and CO/CO₂ mole ratio remained around 1.6 ± 0.4 throughout the pressure range employed.

At an optimum reaction pressure of 15 bar with a feed composition of ethane/air/steam: 27.6/47.6/24.8 mol %, oxidation experiments were carried out at different reaction temperatures in the range of 260-340 °C. The variation in the

selectivity of ethylene, acetic acid, CO and CO₂ along with the ethane conversion as a function of temperature is shown in Figure 8. The ethane conversion at 270 °C was 5 % and increased to 27 mol % at 340 °C. Although the combined selectivity to ethylene and acetic acid was around 80 % throughout the temperature range employed, the acetic acid selectivity decreased from 44 % to 36 % on increasing the temperature from 260 to 340°C. On the other hand, the trend for ethylene selectivity was reverse with increase in temperature. The other products were namely CO and CO₂ increase with temperature due to the combustion reactions of ethylene and acetic acid. The CO selectivity was slightly higher than that of CO₂ as shown in the Figure [24].

The time on stream study was carried out with MoVAIO_x-2 catalyst to test the stability and activity of the catalyst with time. The reaction was carried out for 50 h and was monitored at regular time intervals at 300 °C and 15 bar with the feed ethane/air/steam: 27.6/47.6/24.8 mol %. The profile of ethane conversion and the product selectivity with time is given in Figure 9 where each data point was the average of three experiments.

The influence of addition of water (steam) co-feed on the ethane conversion and the product selectivity was studied at the reaction temperature, 300 °C by varying the partial pressure of water at a constant partial pressure of ethane and oxygen. The ethane conversion and selectivity of the products namely acetic acid, ethylene and CO₂ are shown in Figure 10 as a function of partial pressure of water. The experiment was performed by varying the partial pressure of water between 1.55 to 6.23 bar at a constant total pressure of 15 bar at the reactor inlet where the partial pressure of ethane was 3.22 bar and that of oxygen were 5.63 bar (balance by nitrogen). As shown in the Figure, the conversion of ethane decreases gradually from 23.8 mol % to 16.1 mol % when the partial pressure of water was increased from at 1.55 to 6.23 bar. Addition of steam showed a positive influence on the acetic acid selectivity as the acetic acid selectivity increased from 36.1 mol % at 1.33 bar to 43.9 % at 6.23 bar partial pressure of water whereas ethylene selectivity showed an opposite trend, 41.8 % at 1.33 bar and 37 % at 6.23 bar. The CO₂ selectivity was almost constant for the entire range of water partial pressure where CO was seen only in traces.

Table 2: Selective oxidation of ethane over MoVAIO_x catalysts prepared at different pH values.

Catalyst	Ethane Conversion (mol %)	Product selectivity (%)				CH ₃ COOH Yield (mol %)
		CH ₃ COOH	CH ₂ CH ₂	CO	CO ₂	
MoVAIO _x -1	9.7	30	32	19	19	2.91
MoVAIO _x -2	23	40	40	12	8	9.25
MoVAIO _x -3	10.5	36	46	10	8	3.78
MoVAIO _x -4	8.2	3	18	9	70	0.25

Reaction conditions: Pretreatment temperature: 400 °C for 4 h in He stream (20 ml/min). Reaction conditions: temperature = 300 °C, pressure= 15 bar, ethane = 13.33 ml/min, air = 23 ml/min, steam = 12 ml/min

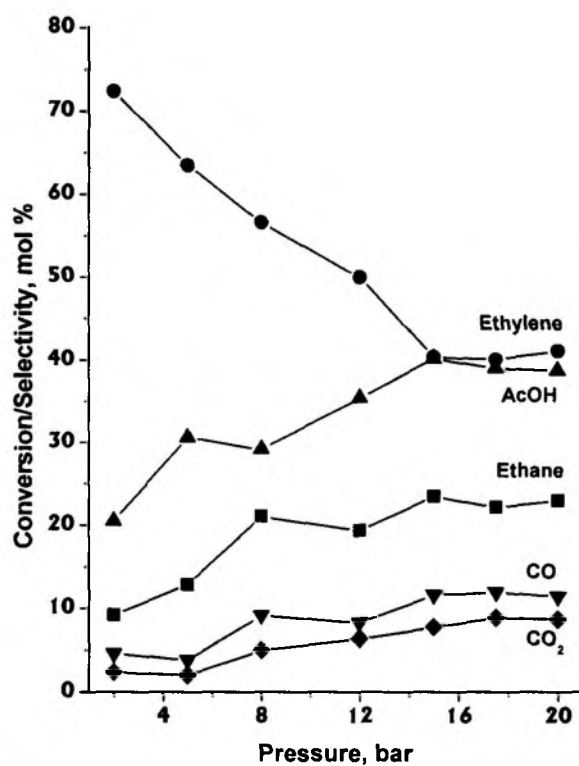


Figure 7: Conversion and selectivity profiles on selective oxidation of ethane over MoVAIO_x-2 catalyst with reaction pressure. Pretreatment temperature: 400 °C for 4 h in He stream (20 ml/min). Reaction conditions: temperature = 300 °C, ethane = 13.33 ml/min, air = 23 ml/min, steam = 12 ml/min

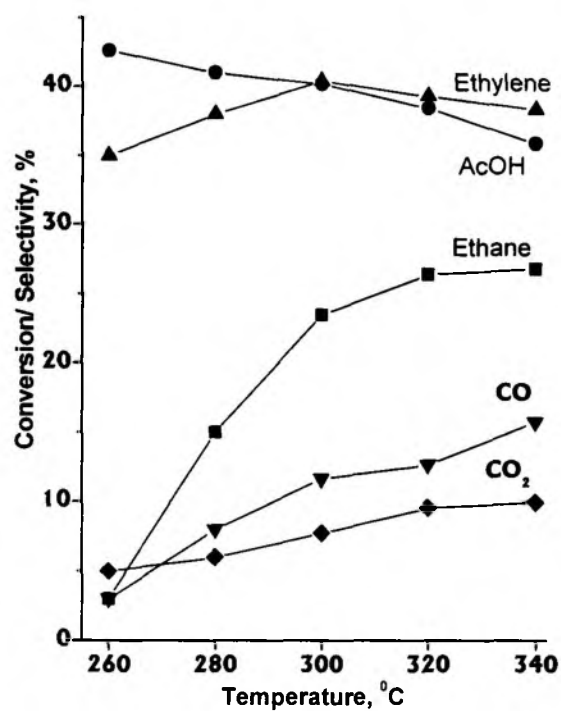


Figure 8: Conversion and selectivity profiles on selective oxidation of ethane over MoVAIO_x-2 catalyst with reaction temperature. Pretreatment temperature: 400°C for 4 h in He stream (20 ml/min). Reaction conditions: pressure= 15 bar, ethane = 13.33 ml/min, air = 23 ml/min, steam = 12 ml/min

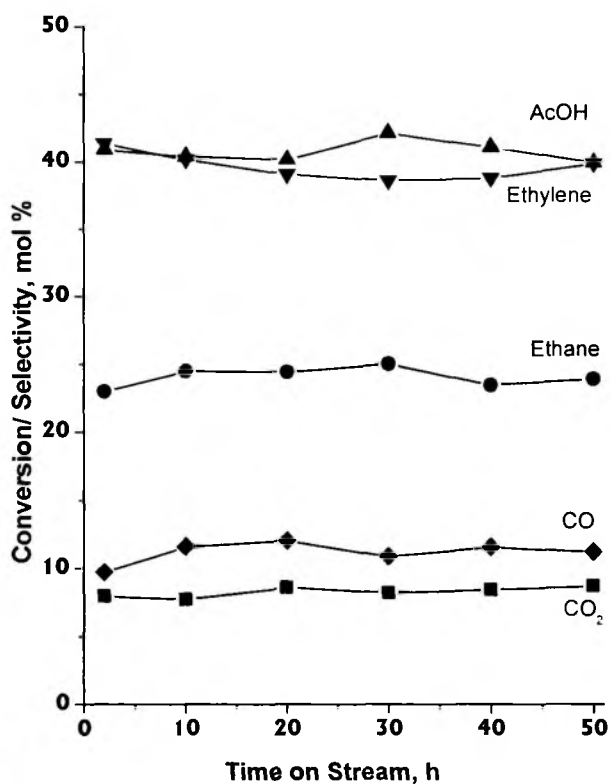


Figure 9: Time on stream study of selective oxidation of ethane over MoVAIO_x-2 catalyst with reaction temperature. Pretreatment temperature: 400°C for 4 h in He stream (20 ml/min). Reaction conditions: temperature = 300 °C, pressure= 15 bar, ethane = 13.33 ml/min, air = 23 ml/min, steam = 12 ml/min

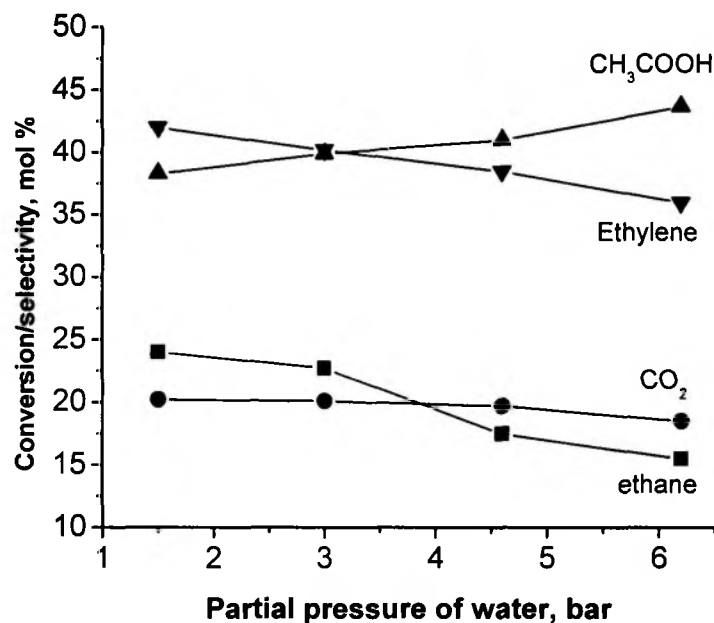


Figure 10: Effect of partial pressure of water on the ethane conversion and product selectivity during selective oxidation of ethane over MoVAIO_x-2 catalyst. Experimental conditions: temperature, 300°C; total pressure, 15 bar; catalyst, 2 g; $PO_2 = 5.625$ bar and $PC_2H_6 = 3.22$ bar, the partial pressure of water was varied between 1.55 to 6.23 bar, total pressure = 15 bar

5.4 Discussion

Although the initial preparative elemental compositions were same, the pH at which the catalysts were made has a strong influence on the bulk and surface elemental compositions and the catalyst yield. Decreasing trend of Mo/V and Mo/Al ratios with increase in pH (Table 1) indicates that Mo content in the catalysts decreases with increase in the pH value. Also, the yield of the calcined catalysts decreased with increase in pH.

The decrease in the Mo content and the catalyst yield should be associated with the higher solubility of Mo or dissociation of Anderson heteropoly compound, $(NH_4)_3AlMo_6H_6O_{24} \cdot 7H_2O$, at higher pH which creates a less favorable situation for the formation of mixed metal oxides with the expected elemental composition. Thus, the pH of the slurry has a profound effect on the nature of the precursors and their amount available for the formation of mixed metal oxide catalysts at the hydrothermal

condition and also on the formation of crystalline phases during the heat treatment as seen in the powder XRD patterns. While the surface area in the range 7-20 m²/g is typical for the mixed metal oxide catalysts, observed lower surface area of MoVAIO_x-1 should be due to its highly crystalline nature [7].

The powder XRD patterns of the present MoVAIO_x catalysts are different from that of the reported MoVAIO_x having a similar elemental composition [25]. The reported XRD pattern of MoVAIO_x showed mainly two sharp peaks at $2\theta = 22$ and 45° (001) reflections along with other diffractions at lower angles. The presence of strong peak line at $2\theta = 22^\circ$ ($d = 4 \text{ \AA}$) was reported to be responsible for the good catalytic activity of the catalyst. However, with the present catalyst systems the peak at $2\theta = 22^\circ$ is not strong. The difference in the XRD patterns of the present catalysts from the reported one may be attributed to the pH condition of the preparative composition and subsequent temperature treatments. All the four as-synthesized catalysts prepared at different pH values were calcined under the identical conditions *i.e.* heating up to 350 °C under static air and then to 400°C under the N₂ atmosphere. α -MoO₃ phase which is present in MoVAIO_x-1 and MoVAIO_x-2 is totally absent in the other two catalysts prepared at higher pH values. Thus, the present results show that the amount of MoO₃ can be controlled by pH of the initial preparative slurry. The presence of high amount of V₂O₅ in MoVAIO_x-4, MoO₃ in MoVAIO_x-1 and different elemental compositions at different pH conditions indicate that presence of the right amount of different elements during the temperature treatment is highly important for the formation of active species. It is generally observed that presence of additional metal ion like Nb to Mo_yV_zO_x basic composition influences formation of partially reduced phase (Mo₄O₁₁ type) and decreases the formation of MoO₃ [26]. It appears that in the present catalyst systems, Al ion plays a role of Nb in stabilizing different active phases. Although Al containing phases are not observed except in MoVAIO_x-4, Al might have been incorporated in vanadomolybdate or highly dispersed on the other phases, owing to its low content such that it is not seen in XRD pattern, or it existed in an amorphous state.

A partial reduction of the catalysts with a temperature treatment is generally observed in the presence of oxalate and nitrate anions in the catalyst precursors [4, 27]. In some cases, the presence of NO_x favors partial oxidation of metal ions with an enhanced activity [28]. Although neither oxalate nor nitrate salts were used in the

present catalyst systems, observed partial reduction of Mo⁶⁺ to Mo⁵⁺ might be due to ammonium ions present. The observation of EPR signal upon the heat treatment of a diamagnetic Mo₆Al-AS precursor substantiates the point that ammonium ions present in the precursor is responsible for the partial reduction of Mo⁶⁺. Estimation of amount of V⁴⁺ and Mo⁵⁺ in the calcined catalysts showing V⁴⁺/V_{total} ~ 0.8 % and Mo⁵⁺/Mo_{total} ~ 2.5 % indicated that majority of Mo and V are in their higher oxidation states, viz., Mo⁶⁺ and V⁵⁺ respectively which are diamagnetic. It may also be noted here that any paramagnetic centers connected through a super exchange pathway leading to strong antiferromagnetic interactions might not have contributed for the EPR intensity. Presence of such antiferromagnetic interactions in the present case can not be ruled out while all the catalysts prepared at different pH values were found to be active for the ethane oxidation as seen in the Table 1, the catalysts prepared at pH 1, 2 or 3 showed better selectivity to ethylene and acetic acid, with a moderate ethane conversion.

Based on the phases identified from the powder XRD, it appears that the MoV₂O₈ phase, which is present in the catalysts prepared at pH 1-3, are possibly responsible for the selective oxidation of ethane to acetic acid/ethylene. The XRD patterns of both MoVAIO_x-1 and MoVAIO_x-2 are nearly similar except for the fact that (020) reflection of MoO₃ is very strong (100 %) in MoVAIO_x-1 as compared to MoVAIO_x-2. The above observation is likely due to the preferential orientation of the MoO₃ crystals in MoVAIO_x-1.

The superior activity of MoVAIO_x-2 compared to MoVAIO_x-1 needs further investigations. The higher ratio of MoV₂O₈/MoO₃ in MoVAIO_x-2 compared to MoVAIO_x-1 may be due to the lower Mo/V ratio in MoVAIO_x-2. As seen in the elemental analysis data (Table 1) the Mo: V ratio was 1:0.15 in MoVAIO_x-1 compared to 1:0.34 in MoVAIO_x-2. The presence of MoV₂O₈ and Mo₄V₆O₂₅ in MoVAIO_x-3 and its moderate activity substantiate the conclusion that MoV₂O₈ might be an important phase responsible for the catalytic activity. The higher ethane conversion with the MoVAIO_x-2 catalyst compared to the MoVAIO_x-3 catalyst indicates that MoO₃ support is important for the better activity.

Apart from MoV₂O₈/MoO₃ ratio, the amount of the reduced phase Mo₄O₁₁ was higher in MoVAIO_x-2 compared to MoVAIO_x-1 indicating the possibility that the MoV₂O₈ phase along with the reduced species may be important for the excellent activity. It may also be noted here that the surface area of MoVAIO_x-2 is higher than

MoVAIO_x-1 which may have some influence on the overall activity of the catalyst. With the above background, it is easy to understand the least catalytic activity of MoVAIO_x-4 catalyst where MoV₂O₈ and Mo₄O₁₁ phases are minor phases and MoO₃ phase was totally absent. Presence of V₂O₅ and other high vanadium containing phases like MoVAIO₄ might be responsible for the over oxidation of the formed product namely ethylene and acetic acid.

It may be noted here that the partial reduction of catalyst precursors has been reported to have a positive influence on the activity and selectivity in selective oxidation of the lower alkanes, though the exact role of these species are yet to be understood [4, 26, 27]. The presence of reduced species with V⁴⁺ centers in MoVAIO_x-1 and MoVAIO_x-2 catalysts and Mo⁵⁺ in MoVAIO_x-3 and MoVAIO_x-4 catalysts is obvious from EPR results. However, the nature and location of V⁴⁺ is not clear from the present study. One possibility is that part of vanadium ion in MoV₂O₈ is in V⁴⁺ oxidation state as MoV₂O₈ is the only vanadium containing crystalline phase in MoVAIO_x-1 and MoVAIO_x-2. However, the absence of V⁴⁺ EPR signal in MoVAIO_x-3 where MoV₂O₈ phase is the major phase does indicate the presence of V⁴⁺ containing non-crystalline species can not be ruled out. Presence of Mo⁵⁺ and other reduced phases containing Mo⁵⁺ are clear from EPR, UV-visible and XRD data.

Thus, we believe that ethane is converted to ethylene by oxidative dehydrogenation mechanism which in turn is adsorbed back on the catalyst to form acetic acid. Decrease in the acetic acid selectivity and increase in the ethylene selectivity on increasing the temperature is believed to be associated with adsorption and desorption phenomena. At high temperatures, the energy, kT (where k is Boltzmann constant) was enough to desorb the ethylene and thus making it not available for the acetic acid formation. The time on stream studies indicated that the catalyst is stable and active for several hours without any deactivation. Commonly occurring catalyst deactivation by coking is not expected in the present systems due to the oxidative experimental conditions. The studies of the effect of partial pressure of water co-feed on ethane oxidation indicated that the water co-feed has a positive influence on the acetic acid selectivity and negative influence on the ethylene selectivity and the ethane conversion rate. The positive influence of steam on the acetic acid selectivity is believed to be associated with the hydroxyl group formation on the surface of catalyst which in turn facilitates the conversion of ethylene to acetic acid [29-31]. A reduction in the rate of ethane oxidation by water co-feed has been

observed by others for various metal oxide systems [2, 8, 29]. The decrease of ethane conversion might be associated with adsorption of strong polar substrate like water and/or acetic acid, thus blocking the active sites that lead to the reduction of the ethane oxidation rate. Different effect of water co-feed on the formation of acetic acid and CO₂ indicates the possibility for different types of sites where water seems to be preferentially interacting on the site that is responsible for ethylene to acetic acid formation.

The efficiency of the present catalyst system for the selective ethane oxidation is assumed to be due to the presence of MoV₂O₈ and other reduced species supported on the MoO₃ phase. Activation of the C-H bond of ethane on the catalytic surface possibly via unstable ethoxy intermediate leads to ethylene formation. Part of the ethylene formed adsorbs either weakly or strongly on the selective site of the catalyst surface in the presence of water and oxygen that leads to the formation of intermediates like ethanol and acetaldehyde and further to acetic acid. Although alcohol/aldehyde products were not seen as major products, their concentrations up to 150 ppm were detected in the GC analysis. With the present experimental conditions, oxidation rate of these alcohol/aldehyde intermediates leading to acetic acid might be very high. Any of these intermediates, ethane and/or acetic acid will be oxidized to CO_x, if they are strongly adsorbed on any non-selective phase (e.g. Al₂O₃ or V₂O₅). Desorption of ethylene will be easier if it is bound on weak acid site like MoO₃.

5.5 Summary and Conclusion

Catalysts of general formula MoVAIO_x prepared with initial elemental composition of 1.00: 0.34: 0.167 (Mo: V: Al) at different pH conditions showed pH dependant elemental compositions. While all of them found to be active for selective oxidation of ethane, catalysts prepared at pH 2 showed excellent activity with 23 % ethane conversion with 80 % combined selectivity to ethylene and acetic acid in equimolar ratio at optimum experimental conditions. From powder XRD and other spectroscopic studies, the high activity is attributed to the presence of MoV₂O₈ and other reduced species like Mo₄O₁₁ phases supported on MoO₃. Although presence of any amorphous phase is not clear at present, presence of V and Mo ions in partially reduced form, as confirmed by Raman, UV-visible and EPR spectra, play a crucial role in the selective oxidation of ethane.

References

1. D. Vitry, Y. Morikawa, J. L. Dubois, W. Ueda, *Appl. Catal. A.* 252 (2003) 411
2. D. Linke, D. Wolf, M. Baerns, O. Timpe, R. Schlögl, S. Zey, U. Dingerdissen, *J. Catal.* 205 (2002) 16
3. M. M. Lin, *Appl. Catal. A.* 207 (2001) 1
4. J. M. Oliver, J. M. L. Nieto, P. Botella, A. Mifsud, *Appl. Catal. A.* 257 (2004) 67
5. Q. Smejkal, D. Linke and M. Baerns, *Chem. Eng. Proc.* 44 (2005) 421
6. J. M. L. Nieto, P. Botella, M. I. Vázquez, A. Dejoz, *Chem. Commun.* (2002) 1906
7. M. Roussel, M. Bouchard, K. Karim, S. Al-Sayari, E. Bordes-Richard, *Appl. Catal. A* 308 (2006) 62
8. E. Heracleous and A.A. Lemonidou, *J. Catal.* 237 (2006) 175
9. S. Zeys, U. Dingerdissen, J. Fritch, US Patent 6,790,983, 2004
10. K. Oshihara, T. Hisano, W. Ueda, *Topics. Catal.* 15 (2001) 153
11. K. Asakura, K. Nakatani, T. Kubota, Y. Iwasawa, *J. Catal.* 194 (2000) 309
12. W. Ueda, N. F. Chen, K. Oshihara, *Chem. Commun.* (1999) 517
13. K. Nomiya, T. Takahashi, T. Shirai, M. Miwa, *Polyhedron* 6 (1987) 213
14. A. Khodakov, B. Olthof, A.T. Bell, E. Iglesia, *J. Catal.* 181 (1999) 205
15. M. Dieterle, G. Mestl, J. Jäger, Y. Uchida, H. Hibst, R. Schlögl, *J. Mol. Catal. A.* 174 (2001) 169
16. G. Mestl, Ch. Linsmeier, R. Gottschall, M. Dieterle, U. Wild, R. Schlögl, *J. Mol. Catal. A.* 162 (2000) 463
17. W. Daniell, A. Ponchel, S. Kuba, F. Anderle, T. Weingand, D.H. Gregory and H. Knozinger, *Topics in Catal* 20 (2002) 65
18. J. M. Jehng, I.E. Wachs, F. T. Clark, M.C. Springman, *J. Mol. Catal.* 81 (1993) 63
19. E. Heracleous, M. Machli, A. A. Lemonidou, I. A. Vasalos, *J. Mol. Catal. A.* 232(2005) 29
20. J. M. Kanervo, M. E. Harlin, A. O. I. Krause, M. A. Bañares, *Catal. Today*, 78 (2003) 171
21. J. M. Oliver, J. M. L. Nieto, P. Botella, *Catal. Today* 96 (2004) 241
22. A. Davidson, M. Che, *J. Phys. Chem.* 96 (1992) 9909

23. E. García-González, J. M. López Nieto, P. Botella and J. M. González-Calbet, *Chem. Mater.* 14 (2002) 4416
24. E. Heracleous, A. A. Lemonidou, J. A. Lercher, *Applied Catalysis A: General* 264
25. K. Oshihara, Y. Nakamura, M. Sakuma, W. Ueda, *Catal. Today* 71 (2001), 153
26. M. Roussel, M. Bouchard, E. Bordes-Richard, K. Karim, S. Al-Sayari, *Catal. Today* 99 (2005) 77
27. H. Tsuji, Y. Koyasu, *J. Am. Chem. Soc.* 124 (2002) 5608
28. A. M. Gaffney, M. D. Heffner, R. Song, EP 1249274 (2002)
29. M. D. Argyle, K. Chen, A. T. Bell, E. Iglesia, *J. Phys. Chem. B* 106 (2002) 5029
30. A. B. Evin, J. A. Rabo, P. H. Kasai, *J. Catal.* 30 (1973) 109
31. J. L. Seoane, P. Boutry, R. Montarnal, *J. Catal.* 63 (1980) 191